Automated Lesion Segmentation in a Marmoset Model of Multiple Sclerosis via Subtraction MRI

Colin Shea[1], Pascal Sati[1], Joseph Guy[1], Emily Leibovitch[1], Steven Jacobson[1], Afonso Silva[1], and Daniel S. Reich[1]
[1]*NINDS, NIH, Bethesda, Maryland, United States*

Target Audience: Pre-clinical scientists, clinicians, image processing scientists.

Purpose/Introduction: To develop an automated algorithm that detects white matter (WM) lesions in a marmoset model of multiple sclerosis (MS). Experimental autoimmune encephalitis (EAE) has been well established in common marmosets as a preclinical research model into the pathogenesis of MS. One difficulty associated with analyzing MRI data is to automatically and reliably detect EAE lesions. Subtraction MRI is a powerful tool to study new lesions in MS, however unique challenges exist for its application in marmoset data due to the lack of equivalent image processing tools. The purpose of the present work is to develop an automated method to segment new white matter lesions from proton density (PDw) and T_2-weighted (T2w) MRI in marmosets using a new brain tissue atlas.

Methods: This animal study was performed on three common marmosets (*Callithrix jacchus*) . These animals were immunized with 200 mg fresh-frozen human WM homogenate emulsified in complete Freund's adjuvant containing 1.8 mg/ml of heat-inactivated *Mycobacterium tuberculosis*. Intradermal injections were divided over four areas: two in the dorsal axillae and two in the dorsal inguinal region. Disease induction was performed at the same time in all animals. In vivo imaging was performed in a 7T/30 cm Bruker scanner (Bruker Biospin, Ettlingen, Germany) using the protocol described previously [1]. Image acquisition was performed pre-immunization (baseline) and at three different time points post-immunization. The imaging protocol included 2D PDw and 2D T2w RARE; nominal in-plane resolution=0.15×0.15 mm; slice thickness=0.6 mm; TR=1700/1200 ms; TE=17/72 ms; FA=90°; echo-train length=1/8; number of excitations=1; AT=7/6 min. Images were processed in the following manner using MIPAV: (a) *Atlas creation* – Baseline PDw scans from four marmosets were co-registered using the FLIRT algorithm with 12 degrees of freedom and averaged to create a PDw brain template. The template brain was manually classified into GM, WM, and CSF in MIPAV using the levelset VOI tool on each slice with manual correction. (b) *Registration* - PDw and T2w scans from all time points were corrected for receive coil inhomogeneity using the N4 algorithm [2] and rigidly registered to the baseline scan. The baseline PD scan was affine registered to the template PD and the transform matrix was inverted and applied to the classification atlas. Each scan was skull-stripped with the registered atlas brain mask and rigidly registered to the skull-stripped baseline image. (c) *Intensity normalization* - Each skull-stripped image was corrected for residual inhomogeneity using N4. The intensity was normalized by creating standard (z) scores relative to the normal-appearing white matter mean and standard deviation using methods described in [3]. (d) *Lesion segmentation* - The normalized PDw and T2w images were averaged together to create a combined P2D contrast for each time point. Each follow-up P2D was subtracted by the baseline P2D and multiplied by the atlas WM mask. The P2D subtraction image was thresholded at 1.5 NAWM standard deviations to create a binary mask and connected components greater than 3 voxels were labeled. The P2D subtraction image was also blurred using a Gaussian filter (σ=1), thresholded at 1.0 NAWM standard deviations, and likewise labeled. Labeled objects that overlapped between the two segmentations were fused and retained while objects that did not overlap were removed. Finally, to compare to a gold standard, lesions were manually segmented using P2D images by a radiologist who was unaware of the results of the automated algorithm.

Results/Discussion: Figure 1 shows derived P2D images from baseline scan (A) and last follow-up scan (B). A representative large, focal lesion is magnified on the subtraction image (C) with corresponding gold standard segmentation (D) and automated segmentation (E). For the three marmosets, manual segmentation detected a total of 198 lesions across all follow-up scans. Comparatively, our method detected 85 true positive lesions, 113 false negatives, and 11 false positives. As shown in Table 1, the true positive (TP) lesions accounted for 79% of the total lesion load. Note these lesions were substantially larger in size than false negatives (FN) and false positives (FP) [mean size (voxels) 97.3 vs. 19.8 and 80.5 respectively]. Small lesions as well as low-intensity diffuse abnormalities (mostly present in marmoset1) constituted the bulk of false negative lesions. Misclassification of white matter as gray matter was also a source of false negatives, mainly located in brain regions where the affine atlas registration insufficient. The primary source of false positive lesions was misregistration between time points which resulted in bright edge artifacts on the subtraction images present in the posterior areas of the monkey brain. Further developments are currently under investigation to reduce false positives and false negatives but our fully-automated method can already robustly detect large focal lesions in marmoset brains.

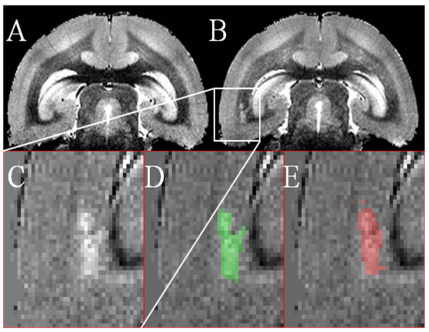

Figure 1. Lesion segmentation. Green: Gold standard. Red: Automated method.

	FP %vol	FN %vol	TP %vol	Lesion Volume
Marmoset 1	26.8%	36.4%	63.7%	27.2
Marmoset 2	10.7%	0.8%	99.2%	18.1
Marmoset 3	2.8%	20.9%	79.1%	96.5
Average	8.4%	21.3%	78.7%	47.3

Table 1. %vol corresponds to % relative to lesion volume from gold standard. All values are the average across the three follow-up scans.

Conclusions: Our initial results indicate that automated skull-stripping, tissue classification, registration, and lesion segmentation are feasible for brain MRI in a marmoset model of MS using an atlas and image subtraction.

References: [1] Gaitan et al., Multiple Sclerosis Journal (2013); [2] Tustison et al., IEEE Trans Med Imaging (2010); [3] Shinohara et al., NeuroImage (2011)